SSRG International Journal of Electronics and Communication Engineering Volume 7 Issue 12, 1-7, December 2020
ISSN: 2348 – 8549 /doi:10.14445/23488549/IJECE-V7I12P101 

# Control of DC-Link Capacitor for Back to Back Converter in Wind Turbine System

Awais Ahmed Memon[#1], Sajid Hussain Qazi[*2], Um-e-Batool[#1]&Muhammad Yasir[#1]

[#1]*Master's Student, Department of Electrical Engineering, Mehran University of Engineering and Technology, SZAB, Campus, Khairpur Mirs', Pakistan*

[#2]*Assistant Prof., Department of Electrical Engineering, Mehran University of Engineering and Technology, SZAB, Campus, Khairpur Mirs', Pakistan*

Received Date: 30 October 2020
Revised Date: 28 December 2020
Accepted Date: 31 December 2020

***Abstract***

*The development of sustainable power sources has opened another skyline to age, transmission, and electrical force distribution. Power electronic converters empower wind turbines, working at changeable speed, to create power further effectively. This study investigates the management of back-to-back converter for doubly fed induction generator in a wind turbine system. The back-to-back converter is an AC-DC-AC converter in which two-stage conversions are required. The first stage is rectification, and the second stage is inversion. The proposed MATLAB/Simulink model's modeling and simulation are focused on a doubly fed induction generator (DFIG) using back to back converter. The controller will be analyzed during the variable wind speed.*

**Keywords** *—Back-to-back converter, DFIG, Wind Turbine, DC-Link capacitor*

## I. INTRODUCTION

Alongside natural advantages of sustainable power sources, innovations in the activity and control of sustainable power sources and the expanding interest for high quality and steady supply bring about more consideration to this energy source. With the advancement of monetary improvement and increment in power requests, the electrical power framework has developed continuously. The interest for new eco-accommodating and financially aggressive techniques for electrical energy generation has expanded in like manner. Along these lines, a renewable power source has become an enormous zone of research. Nowadays, the wind is one of the most encouraging among a few green energetic assets. Wind turbine innovation has been predominant attributable to its ideal specialized and monetary highlights. The basic functions of a back-to-back converter are rectifying the ac source voltage to dc, and the dc is reconverted into ac by inverter. High Voltage Direct Current (HVDC) transmission systems easily control DC power in a short period of time. The back-to-back converter confirms that the outputs are stable [1]. When variations occurred at the load side, then oscillations are produced to the output/load. The speed of the generator varies with the speed of the wind, which will affect the output. When voltage-controlled inverters correspond with synchronous generators, the inverters show poor transient burden sharing, where the inverter gets most of any heap step. This breaking point for the rating of the inverter is comparative with the load step. The primary driver of poor transient burden-sharing is the difference between the inverter and synchronous generator regulation. Nonexistent impedance and transient hang will permit to command over the power-sharing. The exhibition of the DFIG [1] wind turbine framework is magnificent under ordinary voltage conditions. Anyhow, during an even deficiency, high transient flows happen in the stator and rotor windings [1], which straightforwardly influences the machine side converter (MSC) [1], causing harm or upset activity. When an unsymmetrical [1] issue happens, as shown in Figure 1 [2]. The stator's windings have heavy for the short term, and the crooked streams allow the stator's windings to overheat.

Electrical energy is transformed from kinetic energy via doubly-fed induction generators and sent to the grid side through wind energy transformation. Next, a detailed prototype of the wind energy transformation is linked with a changeable speed grid that must be developed to analyze the standard of power at the changeable wind turbine generators' changeable speed, like its connection to the Grid and the numerous system control parameters. There is a wide range of methods for calculating the wind energy conversion system (WECS) taken from the wind. The suggested methods include back to back voltage source converter for wind turbines. The doubly-fed generator model defined throughout the ABC coordinate system will be produced. In addition, the lower order models are often generated from the doubly-fed generator represented in the simultaneously shifting to coordinate system. After that, mathematical equations of 3-phase pulse width modulation, input voltage converters are formed within that ABC coordinate system. The changeable speed of wind turbine generators and both windings of the stator and rotor from doubly-fed induction generators are thoroughly linked to the Grid's side along with the two-way power converter via the slip rings, respectively. A two-way power converter comprises two converters, namely the sides of the stator and rotor. Its dc-link capacitor is situated between both converters. A major goal is to retain the gap of voltage for the DC-link, which is restricted. This is feasible to adjust the torque and the doubly-fed induction generator's path and its real and reactive strength to the stator terminals by managing the rotor side converter. The back-to-back power converters were being regulated in two - way arrangement.

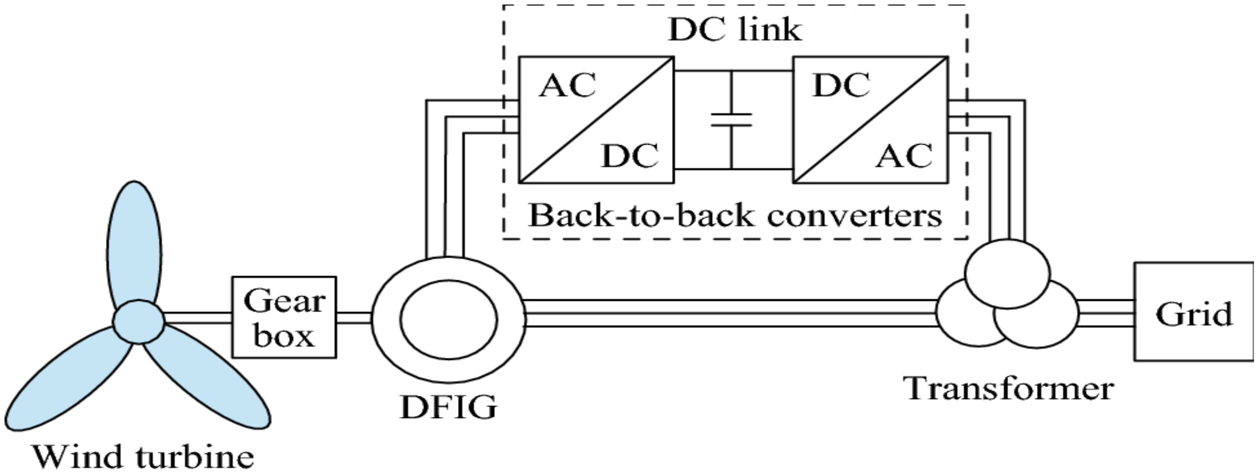


**Fig 01: Block diagram of back to back converter using doubly-fed induction generator in wind turbine**

## II. MODELLING OF DFIG

The DFIG includes windings of rotor and stator composed of three-phase protected coils including fitted accompanied by slip rings. All cables of the stator are linked to the power by a three-phase transformer. The rotor's governed current can be unless pushed into and then drained from the rotor windings by means of certain components. The detailed model of DFIG is given in reference [3]. In a proposed controller of DFIG for the back-to-back converter, the type of generator is the wound rotor induction generator used in the converter modeling.

Generator ratings used in this study of DFIG wind turbine generators for back-to-back converter are seen in table 1 [4].

**TABLE 1**
**Parameters of DFIG Generator**

| | |
|---|---|
| **Rated Power** | 1.5MVA |
| **Stator Voltage** | 575V |
| **Frequency** | 50Hz |
| **Stator Resistance** | 0.01965pu |
| **Stator Inductance** | 0.0397 pu |
| **Rotor Resistance** | 0.01909 pu |
| **Rotor Inductance** | 0.0397 pu |
| **No.of poles** | 06 |

### *a) Proposed Control of Converter*

The two ways power converter comprises two converters, the grid component, the rotor component, and the dc-link capacitor, are positioned in the middle of these two converters. The primary objective of the grid side converter is to preserve the DC-link voltage gap confined. In this study, optimization is taken for the DC-link voltage. The torque, the trajectory of the DFIG, including its real and reactive intensity, can be regulated at the points of the stator by controlling the rotor side converter. It fulfills the unit power factor for the side of the Grid and two-way data energy flow rate. The entire structure's control is configured utilizing the MATLAB/ Simulink software, seen in Figure 2 below. The designed control scheme obtained the simplest and most stable system behavior despite stressing the converters or degrading power efficiency [5].

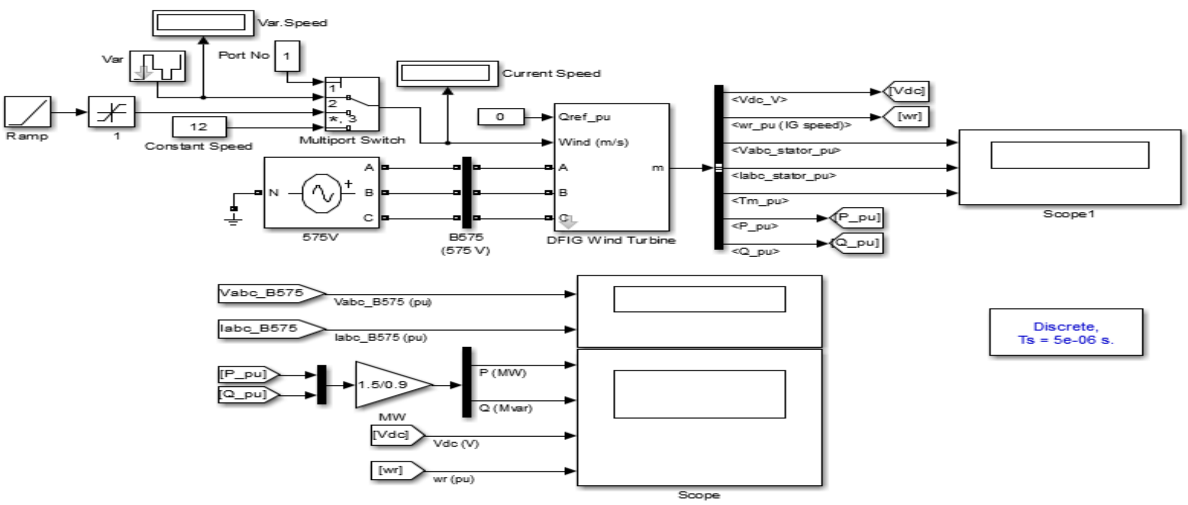


**Fig 02: Proposed Controller in MATLAB/Simulink**

***b) Design of Grid Side Converter***

The type of (DFIG) generator is a wound induction engine with the injection of the rotor. The rate of the DFIG can be regulated by utilizing an adjustable voltage of the slip frequency into the rotor [6, 7]; therefore, it allows optimum energy consumption due to its adjustable speed operation potential [8, 9]. The GSC control system that regulates the voltage through the transfer of reactive power and capacitor in the middle of the Vdc converter and Grid is achieved by changing its current. The DC voltage dynamics in the DC link are now defined in the following paper [9].

***c) Whale Optimization Algorithm (WOA)***

The WOA is a recent community-dependent metaheuristic method proposed by [10] in 2016. The sharks include a single curious functionality such that sharks are known to be among the intellectual creatures. Their minds still have popular spindle cells identical to the brains of humans [11]. Because of such spindle cells, all peoples become a specific organism of the universe, capable of making decisions, desires, and group actions. The sharks have twice quite so many spindle cells as the humans' mind, which is the core of their knowledge. The sharks have a demonstrated capacity to think, understand, assess, interact while becoming reactive as a teenager, but at a smaller degree of awareness. It has already been believed that the bulk of destroyer of sharks can form their specific vernacular. . The greatest marine shark (humpback shark) and teenager shark, almost the area of a bus for school, as well as the popular meat, are krill and tiny fish groups.

***1) Mathematical Formulation For Devising WOA***

To formulate a WOA algorithm, follow the steps of mathematical formulation as detailed in [10].

***2) Encircling Prey Whales***

First, the humpback sharks pinpoint the source and then enclose the meat. In the most portion, the WOA concept implies that the candidate's ideal option is the goal of meat or the way to solve nearest to the optimal hunt negotiator. So, the direction of the optimization process is not defined as the convent. Unless the right choice has been determined, the other sharks (lookup investigators) may attempt to update their specific destination against the right approach. The mathematical connection between sharks enveloping food techniques the governing equations can be stated in [10].

$$\vec{H} = | \vec{E}\overrightarrow{Y^P}(i_1 t) - \vec{Y}(i_1 t) | \quad (1)$$

$$\vec{Y}(i_1\ t+1) = \overrightarrow{Y^P}(i_1 t) - \vec{D}.\vec{H} \quad (2)$$

While (it) denotes the latest repetition, the support implementation for the right approach achieved thus far must be represented by $\vec{Y}$ subject and $\overrightarrow{Y^p}$ subject to the proper position vector; the vector constants $\vec{D}$subject and $\vec{E}$*the* subject can be estimated utilizing the following two equations[10].

$$\vec{E} = 2.r_2 \qquad (3)$$

$$\vec{D} = 2\vec{d}\,r_1 - \vec{d} \quad (4)$$

Where, throughout the steps, the rate of $\vec{d}$ is reduced from 2 to 0. Both amplitudes of $r_1$ and $r_2$ were roughly 0 and 1, respectively, and the governing formula can be stated in$\vec{D}$ is a special variable inside the span of [-$\vec{d}$, d].

## III. SIMULATION RESULTS

The DFIG based wind turbine generator is connected with Grid, and the type of generator and ratings of the generator is already discussed in the above portion.DFIG measured separately at variable speeds to explore the impacts of the capacity harmonic distortion on WTG and at the point of common coupling PCC. A wind turbine is linked in parallel with Grid. The efficiency of the dc capacitor is also inspected at a variable speed of the wind turbine.

In this study, two cases are simulated in MATLAB/Software. The first case is simulated without optimization. The second case is simulated with optimization techniques to get the desired outcomes of the proposed controller. Furthermore, the results will be compared.

***CASE- 1 WITHOUT OPTIMIZATION***

In this case, the proposed controller is run for 15 seconds without utilizing the optimization algorithm to check the proposed controller's performance. The speed of wind varies after 5 seconds in the pattern, as shown in Figure 3. The voltage and current at the stator and rotor side of DFIG are illustrated in Figures 4 and 5, respectively, whereas the voltage and current at the PCC are detailed in Figure 6. The dc-link capacitor's waveform at every instance where the wind speed changes are given in Figure 7.

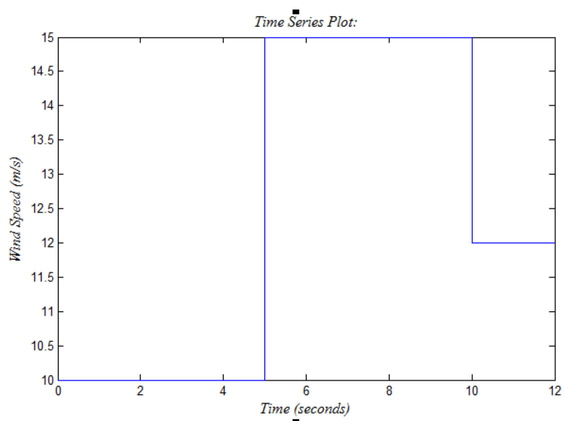


**Fig 03: Speed of Wind Turbine Generator**

The above figure shows that the wind speed is changed after 5 seconds, and its speed is increased from 10m/s to 15m/s at 5 seconds, and 10 seconds speed is decreased to 12m/sec.

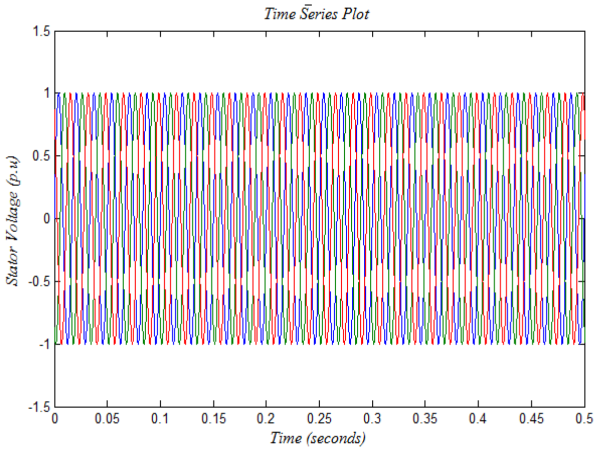


**(a) Stator Voltage**

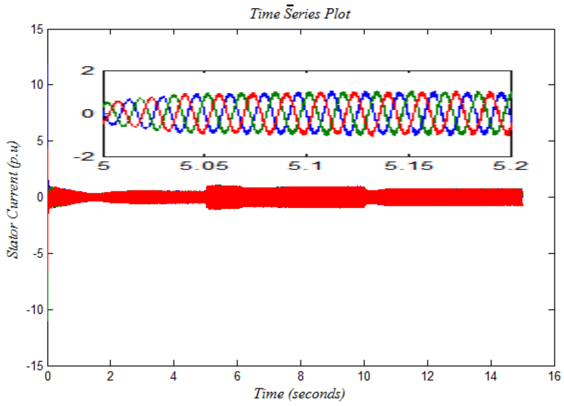


**(b) Stator Current**

**Fig 04: Stator Voltage and Current**

The graphs of stator voltage and stator current are achieved without optimization technique is given in Figure 4 (a) and (b), which shows that the stator voltage remained sinusoidal with the increase and decrease in wind speed whereas, the stator current varies with the increase in speed at t=5 seconds and decrease with the decrease in speed at t=10 seconds. It is obvious from the figure that the stator current stabilized after almost 0.1 sec with an overshoot of 1sec and a rise time of 0.05 sec after the wind speed change.

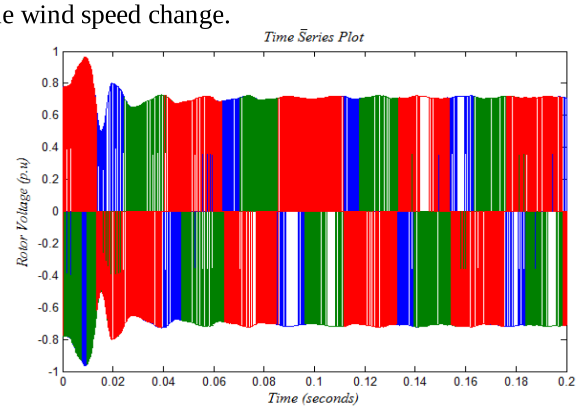


**(a) Rotor Voltage**

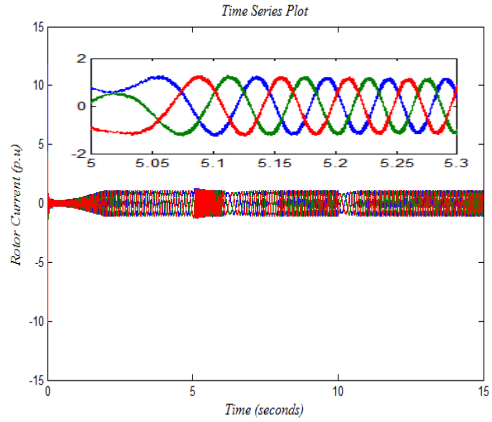


**(b) Rotor Current**

**Fig 05: Rotor Voltage and Current**

The rotor voltage and current of the suggested controller without optimization are displayed in Figure 5 (a) and (b), in which rotor voltage remained sinusoidal with the increase and decrease in wind speed whereas, the rotor current varies with the increase in speed at t=5 seconds and decrease with the decrease in speed at t=10 seconds. It is understandable from the figure that the rotor current stabilized after almost 0.5 sec with an overshoot of 0.5 sec and a rise time of 0.05 sec after the wind speed change.

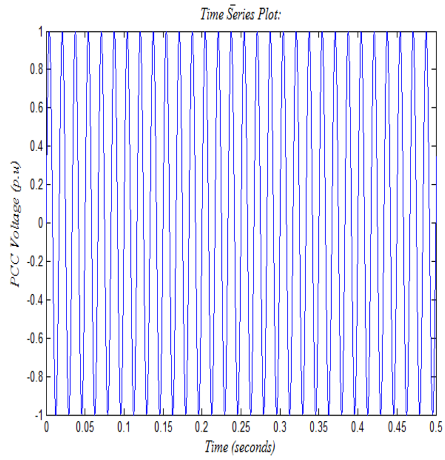


**(a) PCC Voltage**

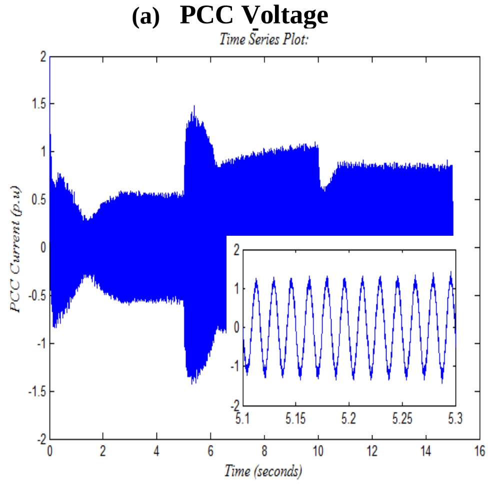


**(b) PCC Current**

**Fig 06: PCC Voltage and Current without Optimization**

The PCC voltage and current of the suggested controller without optimization are displayed in Figure 6 (a) and (b), in which PCC voltage remained sinusoidal with the increase and decrease in wind speed whereas, the PCC current varies with the increase in speed at t=5 seconds and decrease with the decrease in speed at t=10 seconds. It is seen in the figure that the PCC current stabilized after almost 1sec with an overshoot of 1.5 sec and rise time of 0.5 sec after the change in
Wind speed.

Figure 7 the dc-link voltage for the proposed controller is 1150V without utilizing optimization shown in the below figure. During the change in wind speed, dc-link voltage fluctuates and minimizes to 1110V, which is not suitable for the system's optimum operation. Hence, optimization of the dc-link voltage is proposed to maintain the voltage level during any changes in the wind speed.

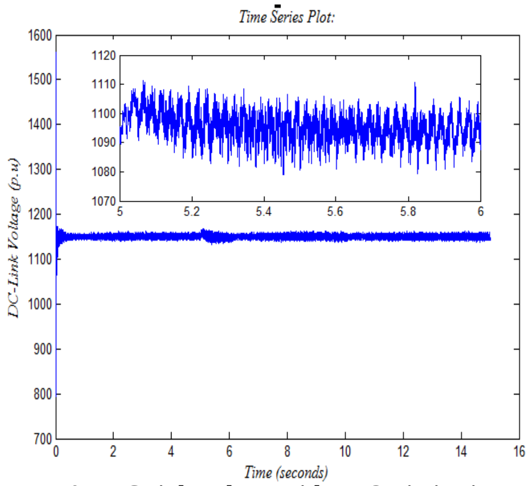


Fig 07: DCLink Voltage without Optimization

***CASE- 2 WITH OPTIMIZATION***

In this case, the proposed controller is run for 15 seconds by utilizing the optimization algorithm to check the proposed controller's performance. The voltage and current at the stator and rotor side of DFIG are illustrated in Figures 8 and 9, respectively, whereas the voltage and current at the PCC are detailed in Figure 10. The fitness functions of optimization which shows in the iteration in Figure 11. The dc-link capacitor's waveform at every instance where the wind speed changes are given in Figure 12.

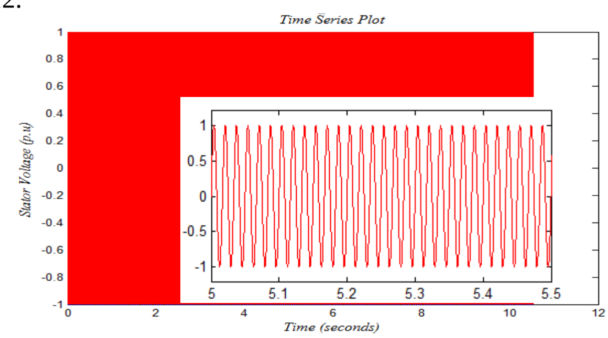


**(a) Stator Voltage**

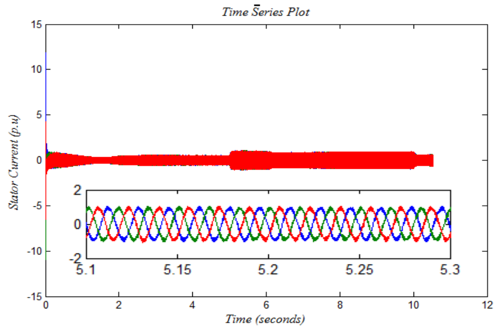


**(b) Stator Current**

**Fig 08: Stator Voltage and Current with Optimization**

The plots of stator voltage and stator current are achieved by utilizing optimization technique is given in Figure 8 (a) and (b), which shows that the stator voltage remained sinusoidal with the increase and decrease in wind speed whereas, the stator current varies with the increase in speed at t=5 seconds and decrease with the decrease in speed at t=10 seconds. It can be seen from the figure that the stator current stabilized after almost 0.2 sec with an overshoot of 0.01sec and rise time of 0.5 sec after the change in wind speed.

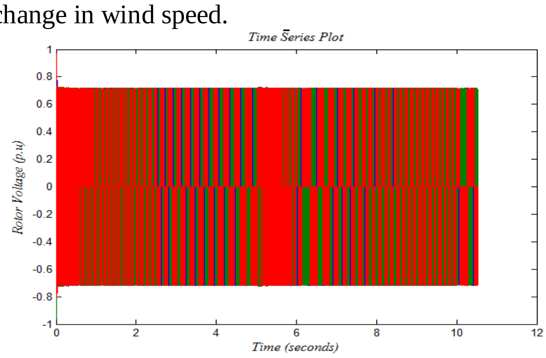


**(a) Rotor Voltage**

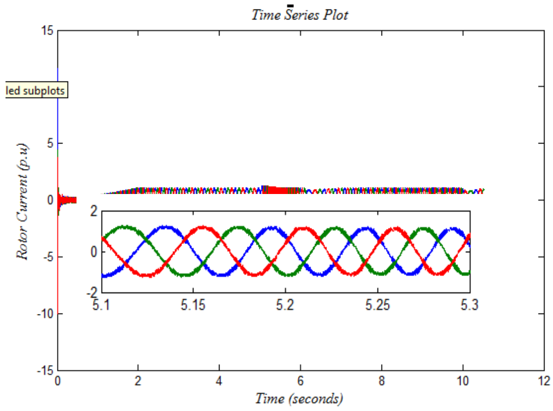


**(b) Rotor Current**

**Fig 09: Rotor Voltage and Current with Optimization**

The rotor voltage and current of the suggested controller with optimization are displayed in Figure 9 (a) and (b), in which rotor voltage remained sinusoidal with the increase and decrease in wind speed whereas, the rotor current varies with the increase in speed at t=5 seconds and decrease with the decrease in speed at t=10 seconds. It is clear from the figure that the rotor current stabilized after almost 1 sec with an overshoot of 0.5 sec and a rise time of 0.5 sec after the wind speed change.

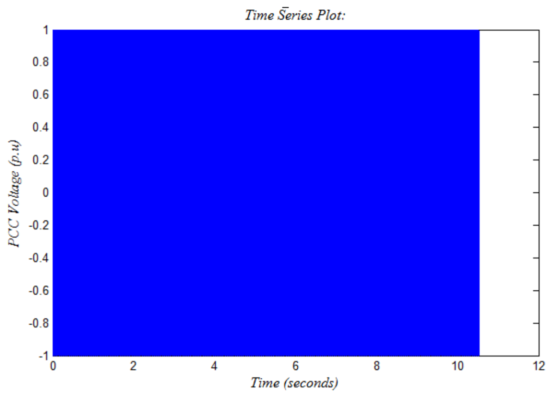


**(a) PCC Voltage**

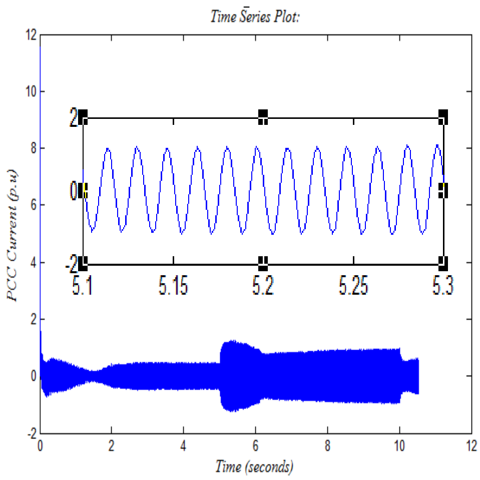


**(b) PCC Current**

**Fig 10: PCC Voltage and Current with Optimization**

The PCC voltage and current of the suggested controller with optimization are illustrated in Figure 10 (a) and (b), in which PCC voltage remained sinusoidal with the increase and decrease in wind speed whereas, the PCC current varies with the increase in speed at t=5 seconds and decrease with the decrease in speed at t=10 seconds. It is seen in the figure that the PCC current stabilized after almost 1 sec with an overshoot of 1.5 sec and rise time of 0.7 sec after the change in wind speed.

The optimization algorithm is run for 100 iterations with 50 search agents. The fitness function achieved from WOA is shown in Figure 11, and it can be witnessed that the WOA algorithm is minimizing the error.

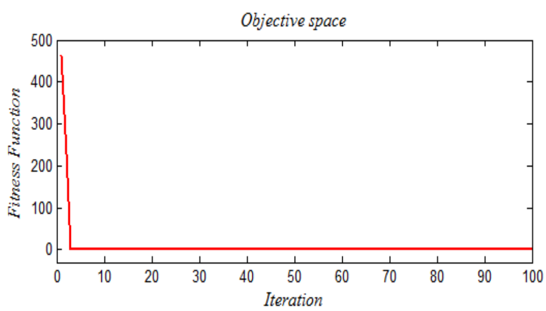


**Fig 11: Fitness Function**

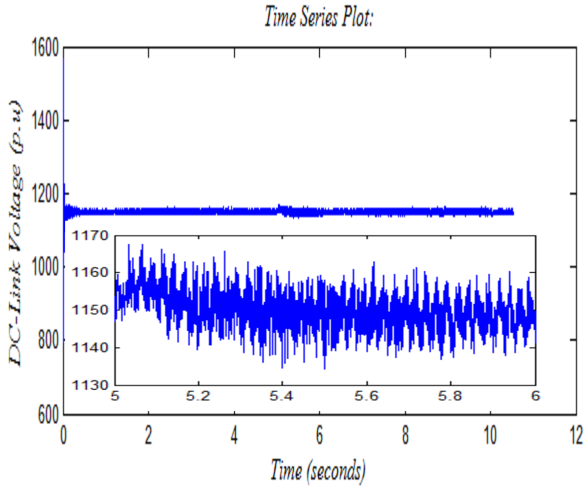


**Fig 12: DC-link Voltage with Optimization**

In Figure 12, the dc-link voltage for a proposed controller is 1150V with utilizing optimization shown in the above figure. During the change in wind speed, dc-link voltage fluctuates and maximizes to 1167V, which is suitable for the system's optimum operation. Hence, the dc-link voltage optimization is proposed to maintain the voltage level during any wind speed changes.

***Comparative Studies***

In this section, a comparative analysis of obtained results from the suggested controller is elaborated. It is evident from the results that the proposed controller with the application of the WOA algorithm provides better results in terms of maintaining sinusoidal waveform at PCC for voltage and current. Additionally, the WOA optimized PI controller's gain values to maintain the DC link voltage to supply the power grid's constant power. The detailed analysis of the obtained results is summarized in Table 2.

**TABLE 2**
**Comparative Analysis**

| Parameters | Controller without optimization | Controller with optimization |
|---|---|---|
| Current Harmonics | 8.5 % | 0.5 % |
| Voltage Harmonics | 12 % | 0.2% |
| Rise Time | 0.7 sec | 0.5 sec |
| Over Shoot | 1.5 sec | 1.5 sec |
| Settling Time | 1 sec | 1 sec |

## IV. CONCLUSIONS

A complete simulation model of the DFIG based wind turbine system is built for the 1.5 MW wind turbine integrated with Grid. Throughout this study, the simulation and regulation of a DFIG based wind turbine-generator system are assumed. Quite precisely, the simulation of the

Multiple components, the optimization techniques for the back-to-back converter have been investigated in depth.

In addition, this study appropriately proposed a back-to-back converter based on WTS Utilizing a DFIG device linked to the Grid. Here, the designed model used the WOA technique to optimize the PI controller's adjustment to the controller's obtained maximum performance. During the optimization technique, the suggested controller utilizing WOA to monitor the goal that is voltage and current.

It is concluded from this study is that the optimization technique performs better results in maximizing the dc voltage to a value of 1167V, which is suitable for the optimum operation of the system during the change in wind speed.

## REFERENCES


[1] Sadara, Wara, and Bunlung Neammanee. Control technique of back - to - back converter for DFIG in wind energy conversion system under abnormal voltage conditions. IEEJ Transactions on Electrical and Electronic Engineering 13, no. 9 (2018) 1285-1295.

[2] Essallah, Sirine, Adel Bouallegue, and Adel Khedher. Integration of automatic voltage regulator and power system stabilizer: small-signal stability in DFIG-based wind farms. Journal of Modern Power Systems and Clean Energy 7(5) (2019) 1115-1128.

[3] T. Senjyu, R. Sakamoto, N. Urasaki, T. Funabashi, H. Fujita, and H. J. I. T. o. E. c. Sekine, Output power leveling of wind turbine generator for all operating regions by pitch angle control, 21(2) (2006) 467-475.

[4] Qazi, Sajid Hussain, and Mohd Wazir Mustafa. Mitigation of Load Harmonics from Grid Connected Wind Turbine: Using Shunt Active Power Filter. Ph.D. diss., Universiti Teknologi Malaysia, 2016.

[5] Karaarslan, A., and Z. Ortatepe. The Grid Side Control of DFIG Based on Wind Turbines. (2016).

[6] Pena, Ruben, J. C. Clare, and G. M. Asher. Doubly fed induction generator using back-to-back PWM converters and its application to variable-speed wind-energy generation. IEE Proceedings-Electric power applications 143(3) (1996): 231-241.

[7] Yanbo, Che, Ren Jingding, Chen Jian, and Chen Xi. Research on grid-side PWM converter based on DSP for double fed wind power generation system. In 2011 4th International Conference on Power Electronics Systems and Applications, (2011)1-6. IEEE.

[8] Zhao, Meihua, Yi Ruan, Yang Shen, Bingying Ye, Qinhong Zhong, and Zhao Meihua. Comparative study of vector control with direct power control for the grid side converter of DFIG wind power generation system. In 2011 International Conference on Electrical and Control Engineering, 3398-3402. IEEE, 2011.

[9] Senapati, Sushanta Kumar, and Ashish Kumar Swain. “Modeling and simulation of AC/DC grid side voltage source converter used in the wind power generation system.” In 2014 International Conference on Circuits, Power and Computing Technologies [ICCPCT-2014] (2014)484-489.

[10] Mirjalili, Seyedali, and Andrew Lewis. The whale optimization algorithm. Advances in engineering software 95 (2016) 51-67.

[11] P. R. Hof, E. J. T. A. R. A. i. I. A. Van der Gucht, E. B. A. i. I. Anatomy, and E. Biology, Structure of the cerebral cortex of the humpback whale, Megaptera novaeangliae (Cetacea, Mysticeti, Balaenopteridae), 290(1) (2007) 1-31.

[12] Ami, Sumit Mazumder. Power quality improvements in low voltage distribution networks containing distributed energy resources. Ph.D. diss., Queensland University of Technology, 2015.

[13] Das, Tapash, Jingxin Zhang, and Hemanshu Pota. A novel performance enhancement scheme for doubly-fed induction generator-based wind power systems under voltage sags and swells. International Journal of Emerging Electric Power Systems 18(4) (2017).

[14] Hilal, Mohamed, Mohamed Maaroufi, and Mohamed Ouassaid. Doubly fed induction generator wind turbine control for maximum power extraction. In 2011 International Conference on Multimedia Computing and Systems, (2011)1-7. IEEE.

[15] Li, Hui, Zhe Chen, and John K. Pedersen. Optimal power control strategy of maximizing wind energy tracking and conversion for VSCF doubly-fed induction generator system. In 2006 CES/IEEE 5th International Power Electronics and Motion Control Conference, 3 (2006) 1-6. IEEE.

[16] Zhou, Dao, and Frede Blaabjerg. Bandwidth-oriented proportional-integral controller design for back-to-back power converters in the DFIG wind turbine system. IET Renewable Power Generation 11(7) (2017) 941-951.

[17] Qazi, Sajid Hussain, Mohd Wazir Mustafa, Umbrin Sultana, Nayyar Hussain Mirjat, Shakir Ali Soomro, and Nadia Rasheed. Regulation of voltage and frequency in solid oxide fuel cell-based autonomous microgrids using the whale's optimization algorithm. Energies 11(5) (2018) 13-18.

[18] Hussain, Musavir, Mazhar H. Baloch, A. H. Memon, and N. K. Pathan. Maximum power tracking system based on power electronic topology for wind energy conversion system applications. Engineering, Technology & Applied Science Research 8(5) (2018) 3392-3397.

[19] Ngom, Ibrahima, Alioune B. Mboup, Abdoulaye Dieng, and Nogaye Diaw. Efficient Control of Doubly Fed Induction Generator Wind Turbine Implementation in Matlab Simulink.

[20] Merabet, Adel, Ahmed Al-Durra, Mahdi Debouza, Aman A. Tanvir, and Hisham Eshaft. “Integral sliding mode control for the back-to-back converter of DFIG wind turbine system.” The Journal of Engineering, 10 (2020) 834-842.

[21] Qazi, Sajid Hussain, Mohd Wazir Mustafa, and Shakir Ali. Review on Current Control Techniques of Grid Connected PWM-VSI Based Distributed Generation. ECTI Transactions on Electrical Engineering, Electronics, and Communications 17(2) (2019) 152-168.

[22] [23] Kumar, M. Satyendra, K. Latha Shenoy, and G. B. Praveen. PWM Techniques to Power Converters of the Wind Energy Conversion System. In 2020 IEEE 9th International Conference on Communication Systems and Network Technologies (CSNT) (2020) 155-160. IEEE.

[23] Car, Mateja, Vinko Lesic, and Mario Vasak. Cascaded control of back-to-back converter DC link voltage robust to grid parameters variation. IEEE Transactions on Industrial Electronics (2020).

[24] Zhang, James-Zhenbin, Tongjing Sun, Fengxiang Wang, Jose Rodriguez, and Ralph Kennel. A computationally efficient quasi-centralized DMPC for back-to-back converter PMSG wind turbine systems without DC-link tracking errors. IEEE Transactions on Industrial Electronics 63(10) (2016): 6160-6171.

[25] Gaber EL-Saady Ahmed, EL-Noby Ahmed Ibrahim and Hazem Hassan Ali"Constant Power Operation Control of Variable Speed Wind Turbine DFIG using Genetic Algorithm", International Journal of Engineering Trends and Technology (IJETT), V37(7),384-393 July 2016.

[26] Saurabh Gupta, S.C. Choube, Sushma Gupta "Voltage Sag-Swell and Harmonics Analysis of UPQC Control Based DFIG- Wind Integration", International Journal of Engineering Trends and Technology (IJETT), V56(1),1-6 January 2018.

[27] V.Krishnamurthy , Ch.Rajesh Kumar. "Constant Power Control Of 15 DFIG Wind Turbines With Superconducting Magnetic Energy Storage System". International Journal of Engineering Trends and Technology (IJETT). V4(9):4193-4200 Sep 2013.

[28] Shilpa Mishra, S Chatterji, Shimi S.L., Sandeep Shukla "Modeling and Control of Standalone PMSG WECS for Grid Compatibility at Varying Wind Speeds", International Journal of Engineering Trends and Technology (IJETT), V17(10),495-501 Nov 2014.